REVIEW OF SCIENTIFIC INSTRUMENTS **89**, 034904 (2018)

Simple and portable low frequency lock-in amplifier designed for photoacoustic measurements and its application to thermal effusivity determination in liquids

Emmanuel Ortega-Robles,[1] Alfredo Cruz-Orea,[2] and David Elías-Viñas[1]
[1]*Sección de Bioelectrónica, Departamento de Ingeniería Eléctrica, CINVESTAV-IPN, A.P. 14-740, 07000 Ciudad de México, Mexico*
[2]*Departamento de Física, CINVESTAV-IPN, A.P. 14-740, 07000 Ciudad de México, Mexico*

(Received 24 July 2017; accepted 6 March 2018; published online 23 March 2018)

The lock-in amplifier is a very useful instrument for observing very small signals under adverse signal-to-noise conditions. In this work, we describe a simple and portable lock-in amplifier designed to be used in photoacoustic measurements. The device was used to measure the thermal effusivity of eight different liquid samples (distilled water, glycerol, acetone, ethanol, 2-propanol, chloroform, hexane, and methanol), as well as the effusivity of acetone in aqueous solution at distinct concentrations, giving good results. The instrument has a bandwidth of 10 Hz–10 kHz and a sensitivity of 1 μV. *Published by AIP Publishing.* https://doi.org/10.1063/1.4997455

I. INTRODUCTION

When measuring, there is sometimes the need to extract a signal of small amplitude from an extremely noisy environment. In most cases, the lock-in amplifier (LIA) is the tool of choice to overcome that situation. This instrument is based on a technique known as phase-sensitive detection.[1] It uses a synchronous demodulator to single out the signal at a specific reference frequency and a narrow band filter to move it back to a direct voltage that is proportional to the original signal amplitude. This way, any other frequency component, such as noise, is rejected.

For this method to work, the signal to be measured must be periodic and frequency-matched with that of the lock-in demodulator. If the phenomenon is not periodic, it can be modulated with the same reference signal of the LIA. If the measured signal is in phase with the reference signal, the output of the lock-in amplifier is directly proportional to its amplitude. Otherwise, it becomes necessary to obtain two orthogonal components to determine the amplitude and relative phase: the in-phase component (I), by demodulating the input signal directly with the reference, and the quadrature component (Q), which results from demodulating it with the reference signal shifted 90°. Then, the amplitude (A) and relative phase (θ) of the original signal can be calculated as $A = \sqrt{I^2 + Q^2}$ and $\theta = \cos^{-1}(Q/A)$.[2]

One of the many cases in which the lock-in amplifier is especially useful is in the application of photoacoustic methods. The photoacoustic effect, discovered by Alexander Graham Bell in 1880 and described mathematically by Rosencwaig and Gersho in 1976,[3] relates to the production of acoustic waves owing to the absorption of pulsed or modulated light in a material. During a regular photoacoustic measurement, a sample of the material of interest is enclosed in a chamber, (photoacoustic cell) while, through a window, a modulated light impinges it at a specific frequency. Some of the energy of this light is absorbed by the material, increasing locally its temperature. This warms up the air layer close to it, generating a periodic pressure variation within the cell that can be converted into an electrical signal (photoacoustic signal) with an appropriate transducer (a microphone or a piezoelectric sensor).

The amplitude of the photoacoustic signal is determined by the thermal and optical properties of the material on which the light strikes (sample), the material behind it (backing), the properties of incident light, and the geometry of the photoacoustic cell.[3] Thus, depending on the experimental setup, different properties can be obtained from either the sample, the backing, or the light source, for example, the optical absorption spectrum of opaque or transparent materials, thermal properties of the sample or backing, and the emission spectrum of the light source.[4]

Unfortunately, most commercially available lock-in amplifiers are bulky and delicate due to their complex design, intended to cover a large number of applications. These devices usually offer large bandwidth, great dynamic reserve, and high phase and frequency resolution. However, the great performance offered by these equipments is in some cases unnecessary due to the research nature, and its use can even result inconvenient for reasons of space or handling. This is why several researchers have chosen to develop their own lock-in amplifiers with specifications that fit their needs. Various papers on these types of developments can be found where analog[5–7] and digital[8–10] lock-in amplifiers are described and recently even embedded in a chip (application-specific integrated circuits).[11–13] By contrast, most of these systems are very specific in their function since they generally work at a fixed frequency and gain and measure either the amplitude or phase but not both magnitudes at a time. The present work aims at giving an intermediate alternative between the very general specifications of the commercial devices and the too particular application of the ones conceived by researchers.

The developed lock-in amplifier was mainly designed to implement photoacoustic experiments in a limited bandwidth, between 10 Hz and 1 kHz, and to measure the amplitude and

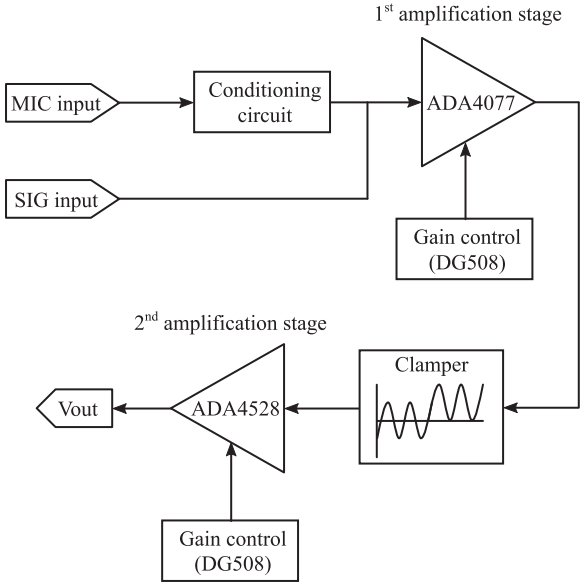

FIG. 1. LIA's input stage diagram.

phase of signals coming primarily from an electret microphone, with magnitudes in the order of millivolts. However, it was decided that the device had a slightly higher bandwidth (10 Hz–10 kHz) and a sensitivity of microvolts so that it could be occupied in other experiments. Furthermore, it was intended to be portable, easy to use, and easily reproducible (with easy to get components and a simple circuit) and that it could send the acquired data to a computer for processing.

II. DESIGN

A. Input stage

The designed LIA has two possible inputs (Fig. 1). One of them has a conditioning circuit to directly connect an electret microphone to the amplifier. The other one goes directly to a first amplification stage. This is performed with a low noise, low offset, and high precision operational amplifier,

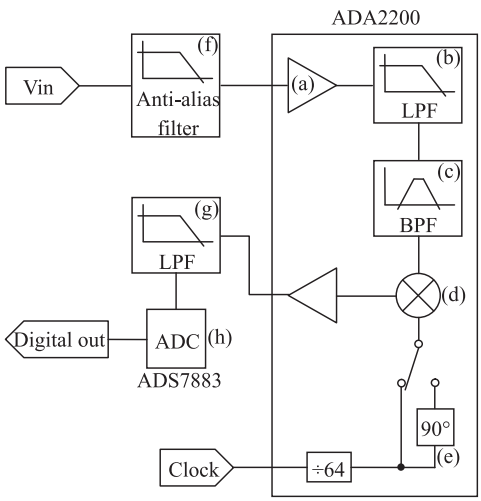

FIG. 2. Synchronous demodulator and analog to digital converter diagram.

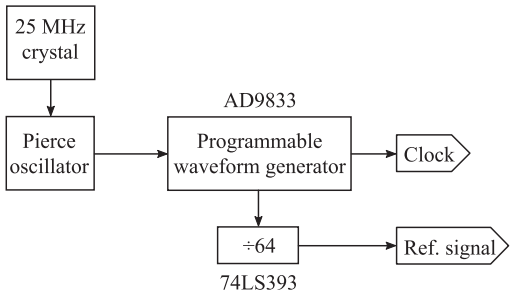

FIG. 3. Programmable waveform generator diagram.

ADA4077, in a non-inverting configuration. Its gain is controlled digitally by means of an analog multiplexer that selects the feedback resistor to achieve gains of 10, 20, 30, or 50. Then, the signal goes through a clamping circuit which adds a voltage level so that it remains always positive. Afterwards, the signal passes to a second amplification stage, similar to the first one but with gains of 2, 4, 10, 20, 40, 100, 300, or 1000. The clamping and second amplification circuits were carried out with a precision ultralow noise amplifier, ADA4528.

B. Synchronous demodulator

Lock-in function itself, namely, that of the synchronous demodulation and bandpass filtering, was accomplished with a single integrated circuit ADA2200. This microchip includes a high impedance input buffer [Fig. 2(a)], a decimation filter which produces one filtered sample for every eight input samples [Fig. 2(b)], a programmable bandpass filter that removes some of the out of band noise [Fig. 2(c)], a mixer that multiplies the filtered signal by the reference to shift its frequency back to DC [Fig. 2(d)] and a phase shifter so that it can be easily obtained the in-phase and quadrature components of the input signal [Fig. 2(e)]. It works only with positive voltages, being that the reason for the previous clamping circuit. Before entering the ADA2200, the signal is passed through a passive filter [Fig. 2(f)] that performs an anti-aliasing function (f_c = 10.6 kHz). The output voltage, which is proportional to one of the orthogonal components of the input signal, depending on the configuration of the phase shifter, was lowpass filtered and then digitalized with a 12-bit analog-to-digital converter (ADC) model ADS7883 [Figs. 2(g) and 2(h)].

The synchronous demodulator chip needs a clock signal which is internally divided by 64 and used as a reference signal for the mixer. This signal was generated with a digitally programmable waveform generator (PWG), AD9833 (Fig. 3). This same signal was also divided 64 times externally by a

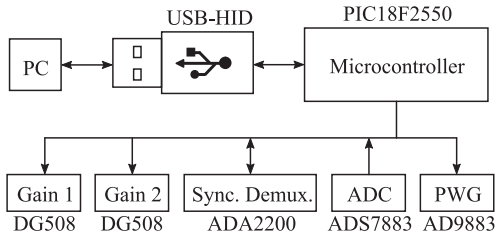

FIG. 4. Microcontroller diagram.

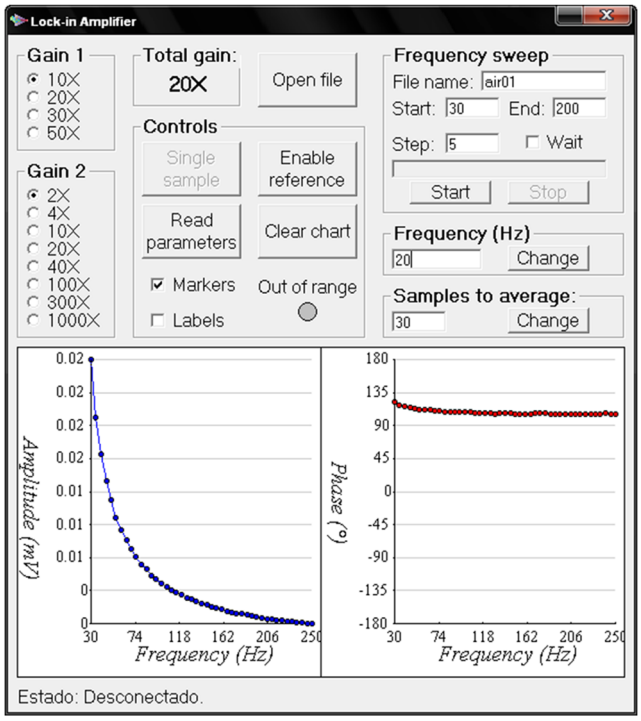

FIG. 5. Graphical user interface.

binary counter, 74LS393, to be used as the reference modulating signal. Although the ideal reference signal should be a sine wave, in practice, a square wave yields to acceptable results and is easier to implement.[14]

C. Control circuit and computer interface

A PIC18F2550 microcontroller was used to control the frequency of the waveform generator, to change the gain selectors, to configure and control the ADA2200, and to read the ADC as well as to establish universal serial bus (USB) communication with a personal computer (PC) (Fig. 4). To this purpose, two programs were written: one for the microcontroller and the other to be used as a graphical user interface (GUI) on the computer. Through this GUI, the operator can control the lock-in functions, make measurements, and save them into text files. Data are displayed in two charts: one for the magnitude and the other for the phase (Fig. 5).

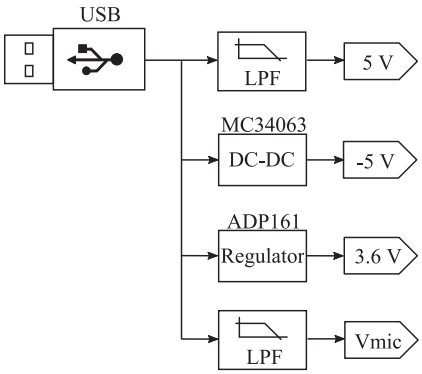

FIG. 6. Power supply diagram.

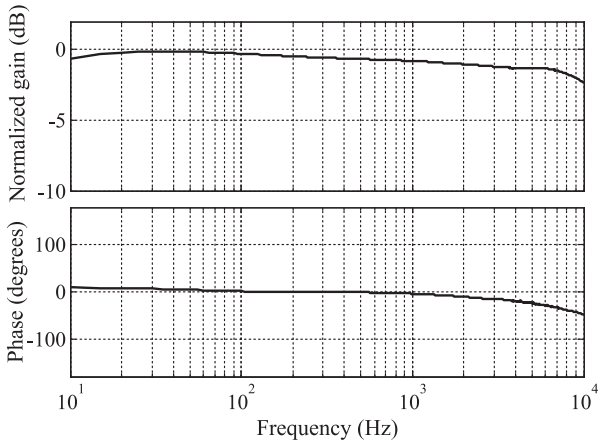

FIG. 7. Frequency response of the lock-in amplifier measured from 10 Hz to 10 kHz.

D. Power supply

The whole system is powered from 5 V of the USB port. A voltage regulator (ADP161) and a DC to DC converter (MC34063) were used to provide the required supply voltages to feed the integrated circuits (Fig. 6). To prevent high frequency noise coming from the computer's switched power supply to affect the measurements, the USB voltage was filtered with a lowpass LC filter ($f_c = 1$ kHz). For the polarization voltage of the electret microphone, a second LC filter was used with a cutoff frequency of 100 Hz. In addition, all components were provided with a decoupling capacitor on the power rails. These filters along with the high power supply rejection ratio (PSRR) of the amplifiers make the system tolerate USB port noise. On the other hand, the lock-in can be plugged to a battery powered laptop, which lowers the power supply noise.

E. Frequency response

Figure 7 shows the frequency response of the lock-in amplifier, both in magnitude and phase. This was measured by connecting a resistive voltage divider directly to the reference output and reading the voltage across the smallest resistance with the unconditioned input (Fig. 8). Then, a frequency sweep from 10 Hz to 10 kHz was performed aided by the lock-in GUI.

III. EXPERIMENTAL

The designed lock-in amplifier was tested in two experiments. In the first one, the thermal effusivity of eight

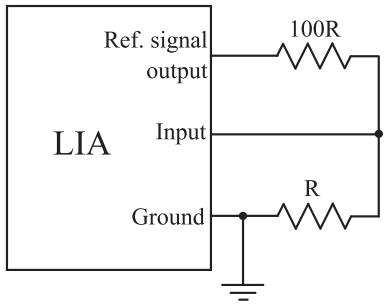

FIG. 8. Circuit used to measure frequency response.

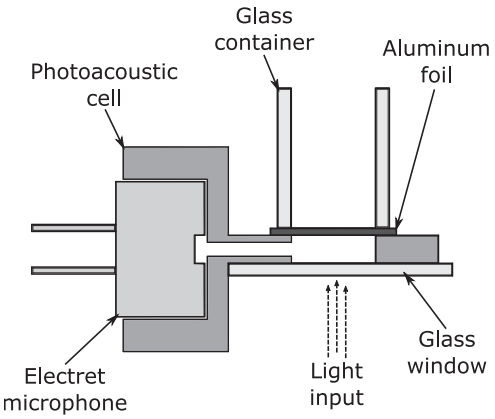

FIG. 9. Diagram of the photoacoustic cell with the sample's container.

liquid samples (distilled water, glycerol, acetone, ethanol, 2-propanol, chloroform, hexane, and methanol) was measured with the method described by Balderas-López *et al.*[15] To this end, a photoacoustic cell was built with the configuration shown in Fig. 9. The electret microphone was connected to the *ad hoc* input of the lock-in amplifier. A 5 W white light-emitting diode (LED) was focused through a glass window on an aluminum foil sample (24 μm of thickness). It was electronically chopped with the aid of a constant current source, driven by the reference signal of the LIA. A glass cylindrical recipient was placed over the aluminum sheet to keep the liquid sample in contact with it. All parts were glued with silicone caulk to maintain the photoacoustic cell hermetically sealed.

For each liquid sample, the amplitude of the photoacoustic signal was registered as a function of the modulation frequency, which varied from 30 to 250 Hz (with increments of 5 Hz), and divided by the amplitude of the photoacoustic signal taken with no sample in the container (air as backing). This ratio R of amplitudes was fitted to the equation[15]

$$R = \left[1 + (b/x) + 0.5(b/x)^2\right]^{-0.5}. \quad (1)$$

In that equation, $b = \varepsilon_s/\varepsilon_{Al}$ is the ratio of the sample to the aluminum thermal effusivities and the quantity x is defined by $x = l_{Al}\sqrt{\pi f/\alpha_{Al}}$, where l_{Al} is the thickness of the aluminum sheet (24 μm) and α_{Al}, its thermal diffusivity (0.9728 cm^2/s).[16]

TABLE I. Thermal effusivities measured with the designed lock-in amplifier and literature values.

	Thermal effusivity (W s$^{1/2}$ K^{-1} cm^{-2})		
Liquid sample	Measured	Literature	Reference
Distilled water	0.1416 ± 0.0100	0.1588	15
Glycerol	0.0834 ± 0.0091	0.0934	15
Acetone	0.0525 ± 0.0086	0.0527	15
Ethanol	0.0580 ± 0.0087	0.0567	15
2-propanol	0.0527 ± 0.0095	0.0525	17
Chloroform	0.0383 ± 0.0049	0.0406	15
Hexane	0.0401 ± 0.0063	0.0440	18
Methanol	0.0643 ± 0.0119	0.0636	15

TABLE II. Thermal effusivities of acetone in distilled water mixtures.

Acetone concentration (%)	Thermal effusivity (W s$^{1/2}$ K^{-1} cm^{-2})
0	0.1589 ± 0.0059
10	0.1522 ± 0.0078
20	0.1437 ± 0.0073
30	0.1346 ± 0.0112
40	0.1267 ± 0.0105
50	0.1123 ± 0.0103
60	0.1059 ± 0.0119
70	0.0924 ± 0.0089
80	0.0816 ± 0.0074
90	0.0730 ± 0.0070
100	0.0526 ± 0.0046

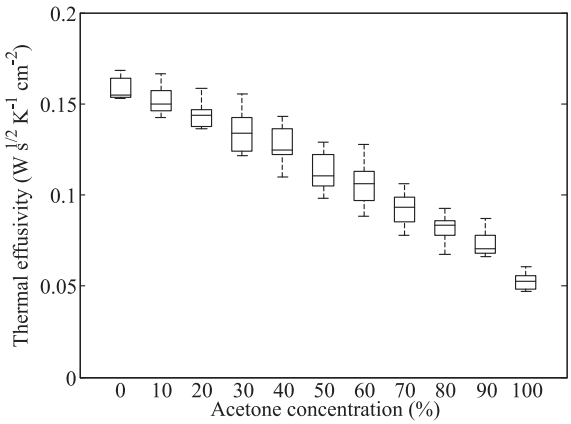

FIG. 10. Thermal effusivity behavior of aqueous solutions of acetone with different concentrations.

As ε_{Al} is known (2.4029 W s$^{1/2}$ K^{-1} cm^{-2}),[16] the sample's effusivity can be calculated from b.

The same experimental setup was used in a second experiment to measure the thermal effusivity of mixtures of acetone in distilled water at different concentrations.

IV. RESULTS

Thermal effusivities were measured as described before for the eight liquids. The results are summarized in Table I and contrasted with values found in the literature.

The results of the second experiment, the thermal effusivity of aqueous solutions of acetone at distinct concentrations, can be appreciated in Table II and Fig. 10.

V. DISCUSSION

It can be seen from Table I that the thermal effusivity values obtained with the proposed LIA are very close to those accomplished by Balderas-López *et al.*[15] with a Stanford Research SR850 lock-in amplifier, and also to the ones of the literature. Moreover, in the second experiment, a clear tendency of the thermal effusivity behavior and concentration can be appreciated.

In Fig. 8, it is shown that the LIA has an almost flat response in the frequency range of 10 Hz–10 kHz. Normalized gain never falls below the −3 dB half-power point and

the phase is almost constant and near zero between 10 Hz and 1 kHz. Although the minimum settable frequency of the waveform generator is 0.1 Hz and the synchronous demodulator can handle low frequencies, the clamping circuit acts as a highpass filter that prevents the measurement of frequencies below 10 Hz. This can be avoided by changing the clamper for other circuits that adds a constant voltage level so that the signal entering the ADA2200 is always positive, but with the drawback that the dynamic range is then reduced. Gain also decays for frequencies above 10 kHz and phase starts to fall above 1 kHz. This is caused by the anti-aliasing filter. It can be easily modified, changing the values of the RC circuit, so that the LIA works up to 30 kHz, which is the bandwidth limit for the ADA2200. However, this filter was set to 10 kHz to help reduce high frequency noise and because the full bandwidth was not required for the photoacoustic experiments to which the LIA is intended.

The lock-in amplifier was able to measure signals with a SNR (signal-to-noise ratio) of −25 dB at a gain of 20 and up to −60 dB at a maximum gain of 15 000, tested at 1 kHz with 10% of accuracy.

The ideal maximum amplitude sensitivity of the LIA is 18 nV, taking into account that the maximum gain of the amplification stage is 50 000, the dynamic range of ADA2200 is 3.6 V, and the ADC is 12 bits of resolution. However, it was experimentally measured to be approximately of 1 μV due to intrinsic noise and especially due to parasitic offset voltages. To achieve better results, amplifiers with lower noise and offset voltage can be used and, in addition, a voltage correction circuit. Also a DC-DC converter may be implemented to ensure a regulated 5 V supply reducing system noise. Nevertheless, the LIA is still sensitive enough to achieve satisfactory performance in many photoacoustic experiments.

VI. CONCLUSIONS

A lock-in amplifier with optimum characteristics was designed for use in experiments with photoacoustic techniques. Its performance was probed in two experiments in which thermal effusivities of different liquid samples were successfully measured. Although the bandwidth of the presented device is limited from 10 Hz to 10 kHz, it can be easily modified to achieve a bandwidth from 0.1 Hz to 30 kHz. Given that the number of electronic components is reduced and the power supply and user interface is given by a personal computer, the proposed LIA is light and portable. The cost of the materials used to build the LIA makes it a reasonable option for research where the budget is significantly constrained.

In addition to its intended application in photoacoustics, this instrument can also be used in other research areas where the characteristics of the equipment are sufficient, such as in precision electrical measurements,[9,19] in other photothermal techniques,[20] in the instrumentation of biosensors,[21] and in Raman thermometry,[22] and even for educational purposes.[23]

ACKNOWLEDGMENTS

The authors would like to thank CONACyT (Mexico) for supporting this work.

[1] A. Cifuentes and E. Marín, Measurement **69**, 31 (2015).
[2] L. Orozco, Analog Dialogue **48**, 1 (2014).
[3] A. Rosencwaig and A. Gersho, J. Appl. Phys. **47**, 64 (1976).
[4] A. Rosencwaig, Opt. Commun. **7**, 305 (1973).
[5] M. Gabal, N. Medrano, B. Calvo, P. A. Martínez, S. Celma, and M. R. Valero, Procedia Eng. **5**, 74 (2010).
[6] P. Vacas-Jacques, J. Linnes, A. Young, V. Gerrard, and J. Gomez-Marquez, Rev. Sci. Instrum. **85**, 033103 (2014).
[7] X. Chen, J. Chang, F. Wang, Z. Wang, W. Wei, Y. Liu, and Z. Qin, Photonic Sens. **7**, 27 (2017).
[8] M. Andersson, L. Persson, T. Svensson, and S. Svanberg, Rev. Sci. Instrum. **78**, 113107 (2007).
[9] L. E. Bengtsson, Rev. Sci. Instrum. **83**, 075103 (2012).
[10] J. Wang, Z. Wang, X. Ji, J. Liu, and G. Liu, Rev. Sci. Instrum. **88**, 023101 (2017).
[11] G. Ferri, P. De Laurentiis, A. D'Amico, and C. Di Natale, Sens. Actuators, A **92**, 263 (2001).
[12] A. D'Amico, A. De Marcellis, C. Di Carlo, C. Di Natale, G. Ferri, E. Martinelli, R. Paolesse, and V. Stornelli, Sens. Actuators, B **144**, 400 (2010).
[13] P. M. Maya-Hernández, L. C. Álvarez-Simón, M. T. Sanz-Pascual, and B. Calvo-López, Sensors **14**, 15880 (2014).
[14] D. P. Blair and P. H. Sydenham, J. Phys. E: Sci. Instrum. **8**, 621 (1975).
[15] J. A. Balderas-López, G. Gutiérrez-Juárez, M. R. Jaime-Fonseca, and F. Sánchez-Sinencio, Rev. Sci. Instrum. **70**, 2069 (1999).
[16] A. Faghri, Y. Zhang, and J. Howell, *Advanced Heat and Mass Transfer* (Global Digital Press, Columbia, 2010).
[17] J. A. Balderas-Lopez, D. Acosta-Avalos, J. J. Alvarado, O. Zelaya-Angel, F. Sanchez-Sinencio, C. Falcony, A. Cruz-Orea, and H. Vargas, Meas. Sci. Technol. **6**, 1163 (1995).
[18] D. Dadarlat, H. Visser, and D. Bicanic, Meas. Sci. Technol. **6**, 1215 (1995).
[19] S. Park and Y. J. Lee, New Phys.: Sae Mulli **65**, 328 (2015).
[20] A. Dhouib, A. Khalfaoui, M. Bouaïcha, and N. Yacoubi, J. Appl. Phys. **123**, 161508 (2017).
[21] G. Xu, X. Ye, L. Qin, Y. Xu, Y. Li, R. Li, and P. Wang, Biosens. Bioelectron. **20**, 1757 (2005).
[22] C. B. Saltonstall, J. Serrano, P. M. Norris, P. E. Hopkins, and T. E. Beechem, Rev. Sci. Instrum. **84**, 064903 (2013).
[23] S. K. Sengupta, J. M. Farnham, and J. E. Whitten, J. Chem. Educ. **82**, 1399 (2005).